2. Тадқиқот ишида салбий ҳароратларда яхлит темирбетон конструкциялар қуриш учун Оҳангарон ПЦ400 Д20 маркали цемент туридан ва лаборатория шароитида синовдан ўтказилган майда ва йирик тўлдирувчилардан, шунингдек "Beton strong 17" комплекс кимёвий қўшимча қўшиш орқали мустаҳкамлиги юқори бўлган оғир бетон олиш мумкинлиги кимёвий таҳлил натижалари орқали ўрганилди. Тажриба намуналари амалдаги бир қатор стандарт талабларга мос равишда синовдан ўтказилди. "Beton strong 17" комплекс кимёвий қўшимчанинг физик-кимёвий хоссалари ўрганилди ва тадқиқот ишининг кейинги босқичи- лаборатиория шароитида синов намуналарининг таркибини ишлаб чиқиш ҳамда

ушбу таркиблар асосида тайёрланган материалларнинг синов намуналарини тайёрлашда фойдаланиш учун тадқиқот объектлари сифатида танланди.

3.Хом ашё материалларининг физик-кимёвий ва физик-механик хоссалари стандарт ва тадқиқот усуллари бўйича тавсифланди ва амалда қўллаш учун фойдаланилди.

4. Материаллар ишлаб чиқариш технологияси, технологик жиҳозлар, асбоб-ускуналари ҳамда техник ва технологик назоратнинг янги самарадор усулларини ишлаб яиқиш ва жорий этишни мутассил амалга оширишни доимо такомиллаштириб бориш уларни сифатини таъминлашга замин яратади ва кафолатлайди.

Адабиётлар
1. Баженов Ю.М. Технология бетона. М.: Изд-во АСВ, 2003.
2.Шокиров.Т.Т., Усмонова.Д.А. "Кимёвий анализ таҳлилларида комплекс қўшимчаларнинг совуқ ҳароратда бетон хоссаларига таъсири"// Самарқанд "Меъморчилик ва қурилиш муаммолари" илмий-техник журнал. 2022-й. 3-сон.107-110-бет
3. Turgunovich S. T., Asatilloyevna U. D., Qizi S. D. Z. A. THE USE OF CHEMICAL ADDITIVES IN COLD CLIMATES AND THEIR EFFECT ON THE CONCRETE MIXTURE //Трансформация моделей корпоративного управления в условиях цифровой экономики. – 2022. – Т. 1. – №. 1. – С. 107-113

APPLICATION OF MPC-CONTROLLED COHESIVE ZONE MODELING FOR TEXTILE COMPOSITE FAILURE SIMULATION

Visiting Professor KYEONGSIK WOO, PhD (TUACE)

Annotation: *In this paper, an MPC (multi-point constraint)-controlled selective activation method of cohesive elements is applied to simulate the progressive failure of textile composite material. First, cohesive elements are inserted between all bulk element sides in the region where failures may occur. The duplicated cohesive nodes are tied using MPCs prior to the start of the analysis, eliminating all additional degrees of freedom. As the analysis progresses, the MPCs are selectively released for nodes located in the region where failure is predicted to be imminent and, thus, the corresponding cohesive elements are activated. When applied to textile composite failure analyses, the present method demonstrated the accurate prediction of the stress-strain curves as well as the failure progression history while significantly reducing computer memory and computation time compared to those by the conventional cohesive zone modeling method.*

Аннотация: *В этой статье метод выборочной активации когезионных элементов, управляемый МРС (многоточечным ограничением), применяется для моделирования постепенного разрушения текстильного композиционного материала. Сначала между всеми сторонами объемного элемента в зоне возможного разрушения вставляются связующие элементы. Дублированные связные узлы связываются с помощью МРС до начала анализа, исключая все дополнительные степени свободы. По мере проведения анализа МРС выборочно высвобождаются для узлов, расположенных в области, где прогнозируется неизбежный отказ, и, таким образом, активируются соответствующие связующие элементы. Применительно к анализу разрушения текстильных композитов настоящий метод продемонстрировал точное предсказание кривых нагрузки-перемещения, а также истории развития разрушения, при этом*

значительно сокращая компьютерную память и время вычислений по сравнению с традиционным методом моделирования когезионной зоны.

Annotatsiya: *Ushbu maqolada to'qimachilik kompozit materialining progressiv nosozligini taqlid qilish uchun birlashtiruvchi elementlarning MPC (ko'p nuqtali cheklov) tomonidan boshqariladigan selektiv faollashtirish usuli qo'llaniladi. Birinchidan, nosozliklar yuzaga kelishi mumkin bo'lgan mintaqadagi barcha ommaviy elementlarning tomonlari orasiga birlashtiruvchi elementlar kiritiladi. Takrorlangan birlashtiruvchi tugunlar tahlil boshlanishidan oldin MPC yordamida bog'lanadi, bu esa barcha qo'shimcha erkinlik darajalarini yo'q qiladi. Tahlil davom etar ekan, MPClar nosozliklar kutilayotgan hududda joylashgan tugunlar uchun tanlab chiqariladi va shu bilan mos keluvchi elementlar faollashadi. To'qimachilik kompozitsion nosozliklarini tahlil qilishda qo'llanilganda, ushbu usul an'anaviy koheziv zonani modellashtirish usuli bilan solishtirganda kompyuter xotirasi va hisoblash vaqtini sezilarli darajada qisqartirish bilan bir qatorda yukning siljishi egri chiziqlarini aniq prognoz qilishni va nosozlikning rivojlanish tarixini ko'rsatdi.*

Keywords: *Composite failure, progressive failure analysis, cohesive zone modeling, selective activation, multi-point constraint.*

Ключевые слова: *Составной отказ, анализ прогрессивного отказа, моделирование связной зоны, выборочная активация, многоточечные ограничения.*

Kalit so'zlar: *Kompozit nosozlik, progressiv nosozlik tahlili, birlashgan zonani modellashtirish, selektiv faollashtirish, ko'p nuqtali cheklash.*

INTRODUCTION. Over the past few decades, the use of textile composites has continuously increased in aerospace, automobile, marine, and civil engineering structures. Textile composites have interlaced fiber tow architectures that provide superior drapeability, balanced orientation and improved impact resistance compared to unidirectional laminated composites. However, complicated fiber tow structures make analytical studies of mechanical behavior very difficult. For decades, researchers have studied geometrical modeling and mechanical characterization of properties, but many problems remain unsolved, especially in predicting progressive failure behavior [1,2].

Failure analysis of textile composites has been performed using strength methods, virtual crack closure technique (VCCT) and continuum damage mechanics (CDM). Recently, the use of cohesive zone modeling (CZM) for fracture analysis of engineering materials has increased significantly [3,4]. In the CZM method, cohesive elements with traction-separation laws (TSLs) that govern the behavior of the cohesive elements are inserted between regular bulk elements. If a crack propagation path is known, such as delamination failures propagating along particular ply interfaces, a limited number of cohesive elements can be inserted only between bulk elements of the failure propagation paths. In many cases, the failure propagation paths are not known *a priori*, so a large number of cohesive elements have to be fully inserted between all element sides to provide possible failure paths. However, the full insertion can significantly increase the size of the numerical analysis model, as well as lead to the so-called additional compliance problem in which the numerical model appears smoother than the actual structure [5].

The added compliance problem can be eliminated by using extrinsic CZMs with initially rigid TSLs, especially by inserting cohesive elements adaptively as needed during analysis using explicit solvers [6]. For intrinsic CZMs with implicit solvers, however, adaptive insertion is not possible because mesh changes are not allowed, so the aforementioned problem is not resolved. To minimize the added compliance issues, a new strategy was developed for intrinsic CZM using implicit solvers [7]. This method, MPC-controlled CZM, is similar to an adaptive insertion method using explicit solvers. The difference is that instead of adaptively inserting cohesive elements, the cohesive elements are adaptively activated by controlling the MPCs.

In this study, the selective activation of cohesive element strategy by MPC control was developed and applied to the progressive meso-mechanical failure analysis of textile composite unit cells. To apply the selective activation strategy, regular bulk element meshes were generated

first, and the cohesive elements were inserted fully between all element sides before analyses, where all duplicated cohesive nodes were tied by controllable MPCs. During the analysis, the cohesive elements predicted near the start of the failure were activated by releasing the corresponding MPCs. The results indicated that the present strategy accurately predicted the stress-strain curves as well as the failure progression history.

METHODS. (1) FE modeling. This section describes the unit cell modeling of plain weave textile composite. Figure 1 shows the architecture of warp tow and fill tow interlacing with each other. After weaving the tows, the matrix is impregnated to form a plain weave layer.
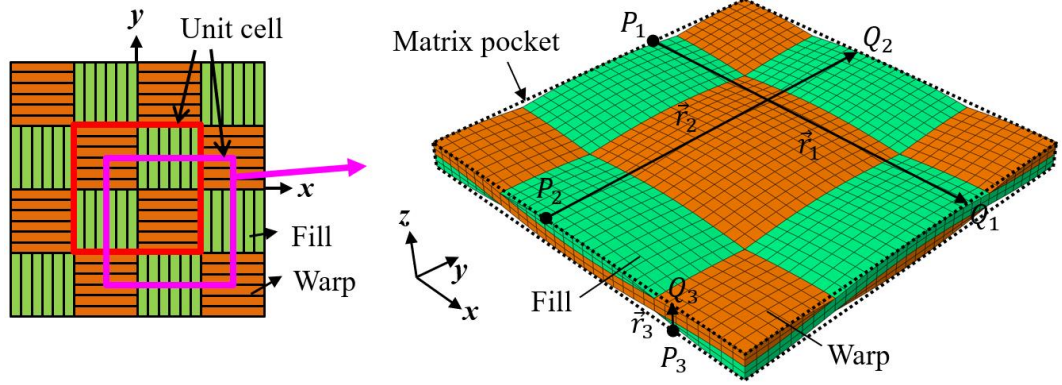
Figure 1. Fiber tow architecture of plain weave textile composites.

The mechanical properties of textile composites are obtained through a series of elastic and fracture tests. However, in many cases, actual tests are time-consuming and costly, and studies have been conducted by many researchers to characterize mechanical behavior analytically. For structures exhibiting repeating pattern such as the textile composites shown in Figure 3, unit cell analysis method can be used for efficient analyses. In this case, the minimum repeating block can be identified as a unit cell, and the repeating pattern of the unit cell can be represented using geometric parameters of warp and fill tows as $\vec{r}_1 = \lambda_w \vec{e}_x, \vec{r}_2 = \lambda_f \vec{e}_y, \vec{r}_3 = h\vec{e}_z$. Here, $\vec{r}_\alpha$ ($\alpha = 1,2,3$) is the periodicity vector where λ_w and λ_f denote the wavelengths of the warp and fill tows, respectively. The ply thickness (h) is the sum of warp, fill, and matrix thicknesses ($h = t_w + t_f + t_m$). In addition, all points of the opposing boundary surfaces are expressed as $\vec{P}_\alpha + \vec{r}_\alpha = \vec{Q}_\alpha$. Then, the periodic boundary condition (PBC) can be written as $\vec{u}_{P_\alpha} + \underline{\epsilon}(\vec{r}_\alpha) = \vec{u}_{Q_\alpha}$ for a given nominal strain state. As such, tensile or shear tests can be numerically simulated using unit cells with the periodic boundary conditions.

In this study, X-ray CT imaging was performed on a plain weave textile composite specimen, and geometric parameters were measured by constructing a three-dimensional geometric model through image processing [8]. The measured values of the geometric parameters are $\lambda_w = \lambda_f = 4.476\ mm$, $t_w = t_f = 0.146\ mm$, and $t_m = 0.002\ mm$.

From the unit cell geometric parameters, a three-dimensional finite element mesh for a two-ply unit cell model. Figure 2 shows a quarter of the finite element mesh. While the mesh was generated for the full unit cell region, the mesh for the region $-\lambda_w/2 \leq x \leq \lambda_w/2$ and $-\lambda_f/2 \leq y \leq \lambda_f/2$ is shown in the figure. The finite element mesh consists of regular elements and cohesive elements. The cohesive elements are divided into four groups that model four failure modes: fiber fracture, matrix failure in tows, failure in pure matrix, and interface separation. The regular elements of fiber tows are given fiber tow properties in local element coordinates and the regular elements of pure matrix pocket region are given matrix properties. The cohesive elements are given different cohesive failure properties in response to the failure modes. Table 1 summarizes the material properties used. In this study, the quadratic nominal

stress criterion was used for the failure initiation, and the energy-based failure evolution model for damage propagation with BK-mixed mode criterion [9].
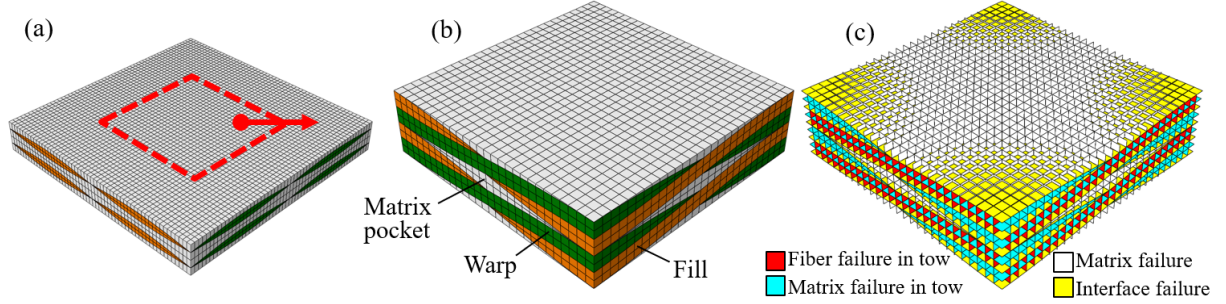
Figure 2. Break-up of finite element mesh: (a) unit cell mesh, (b) regular elements, and (c) cohesive elements.

Table 1. Elastic and cohesive properties.

Elastic property	Fiber tow	$E_{11} = 156\ GPa, E_{22} = 10.4\ GPa, v_{12} = 0.26, v_{23} = 0.44, G_{12} = 5.9\ GPa, G_{23} = 2.8\ GPa$
	Pure matrix	$E = 3.8\ GPa, v = 0.34$
Cohesive property	Fiber failure in tow	$T_1 = 2000\ MPa, G_{IC} = 30\ N/mm$
	Matrix failure in tow	$T_1 = 60\ MPa, T_2 = 90\ MPa, G_{IC} = 0.2\ N/mm, G_{IIC} = 1.3\ N/mm$
	Pure matrix failure	$T_1 = 60\ MPa, T_2 = 120\ MPa, G_{IC} = 0.6\ N/mm, G_{IIC} = 1.0\ N/mm$
	Interface failure	$T_1 = 60\ MPa, T_2 = 90\ MPa, G_{IC} = 0.2\ N/mm, G_{IIC} = 1.0\ N/mm$

(2) MPC-controlled CZM. Figure 3 shows the basic concept of the MPC-controlled CZM (MCZM) in a two-dimensional sense. The figure shows a finite element mesh with 4-regular elements and 4-cohesive elements inserted between the regular elements. The thickness of cohesive elements is numerical zero, but the cohesive elements are plotted as having finite thicknesses for viewing purposes. Initially, the duplicate cohesive nodes are tied using MPCs. For example, in the right zoomed-in plot the two nodes are tied to behave as one node, so initially the analysis gets started as if there are no inserted cohesive elements. During analysis, the stress state of the regular elements is continuously monitored and when a release condition is met (i.e., when an imminent failure is predicted), the MPC ties are released and the corresponding cohesive elements become activated.

The concept of MCZM can also be understood from the perspective of TSL, which governs the behavior of cohesive elements. Figure 4 shows the conventional bi-linear TSL and MPC-modified TSL. Here, δ_0, δ_f, T_{max} and G_c represent failure initiation and completion displacements, maximum traction and fracture energy, respectively. In conventional TSL, the initial elastic slope K gives rise to the added compliance. Using the MPC-modified TSL, the initial elastic effect can be minimized by releasing the MPC when the traction value is near the maximum value, i.e., when $T = T(\tilde{\sigma})$. If $T(\tilde{\sigma}) = 0$, it is the same method as the conventional CZM, and if $T(\tilde{\sigma}) = T_{max}$, it is practically equivalent to the extrinsic CZM.

MPC release traction ($T(\tilde{\sigma})$) can be selected by using failure criteria. In this study, the Hashin failure criterion was used for the release condition. It should be noted that any failure criterion can be used for the release condition because the accuracy of the solution is dependent solely on the TSL of the CZM, not on the failure criterion to release the MPCs.

Figure 3. Schematic of tying and releasing MPCs of cohesive nodes.
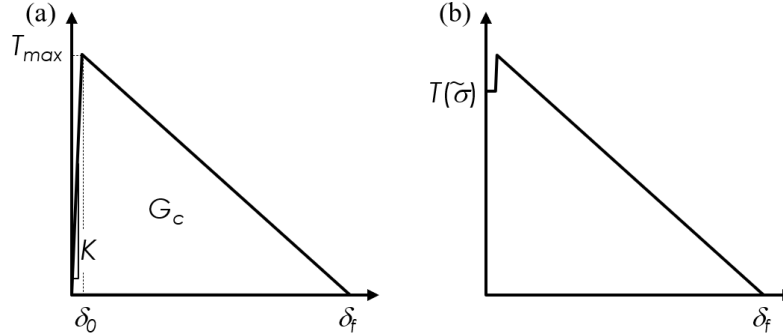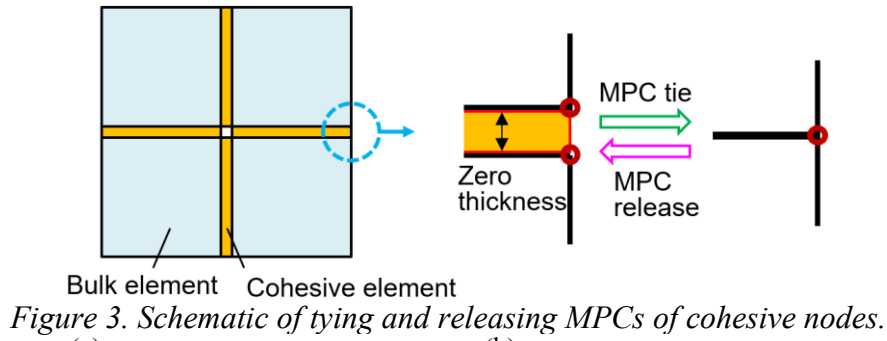
Figure 4. Comparison of TSLs: (a) Conventional TSL, and (b) MPC-controlled TSL

RESULTS and DISCUSSION. (1) Validation of MCZM. The effective elastic modulus (E_{xx}) and failure strength (X_T) calculated by MPC-controlled CZM showed negligible differences. When compared to the experimental data, the results predicted by the present method matched accurately. The differences in E_{xx} and X_T were 0.9% and 17.3%, respectively, which validates the applicability of the present method.

(2) Failure progression history. Figures 5-6 shows the failure progression histories when the uni-axial tension load was applied in the x-direction, simulating the uni-axial tension test. The stress distributions with failure shapes are plotted for the whole unit cell in Figure 5, and only for warp and fill tows in Figure 6. Because warp and fill tows change their fiber direction continuously, the stresses are plotted in the material axis of each element. In the figures, material axes are plotted for example elements of warp, fill and matrix pocket. The nominal stress-strain curve is plotted in Figure 7. Markers *a-e* correspond to the failure states in Figures 5-6.

It can be seen that under the uni-axial tensile load in the x-direction, the first failure occurs fairly early at the warp-fill crossover edges of fill tows when $\bar{\varepsilon}_{xx} = 0.0046$. The failure mode is mainly matrix direction failure dominated by σ_{33} stress. When $\bar{\varepsilon}_{xx} = 0.0066$, the failure in fill tows gradually propagates and the whole fill tows enter into failure process. This failure causes a slope change in the stress-strain curve in Figure 7 between *a* and *b*, which indicates the unit cell structure becomes softened by the failure. For warp tows, the concave region showed a large area of high σ_{11} distribution, whereas fiber direction failures begin at the warp-fill crossover edges of the warp tows when $\bar{\varepsilon}_{xx} = 0.0136$. At this time, the matrix pocket region near the failing warp tow region also starts to fail. The failure in warp tows propagates to a relatively short increase in the applied strain, with the nominal stress σ_{xx} reaching its peak value and then decreasing as seen between *c* and *d* in Figure 7. The fiber failure progresses thru the edge region of warp tows when $\bar{\varepsilon}_{xx} = 0.0148$, after which a very quick failure propagation occurs showing most part of the warp tows is completely failed in Figure 6(e) when $\bar{\varepsilon}_{xx} = 0.0150$. Because the warp tows carry most of the tensile load, the failure of the warp tows drastically reduces the slope of the stress-strain curve between *d* and *e* in Figure 7.
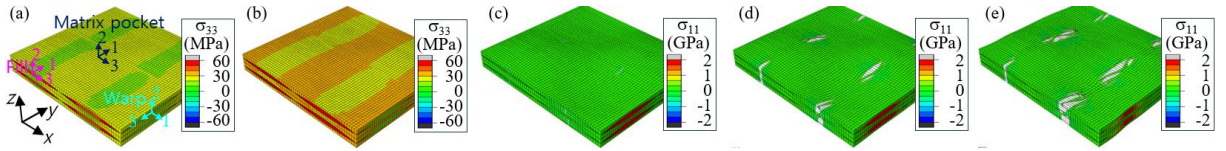
Figure 5. Failure propagation history: (a) $\bar{\varepsilon}_{xx} = 0.0046$, (b) $\bar{\varepsilon}_{xx} = 0.0066$, (c) $\bar{\varepsilon}_{xx} = 0.0136$, (d) $\bar{\varepsilon}_{xx} = 0.0148$, and (e) $\bar{\varepsilon}_{xx} = 0.0150$.
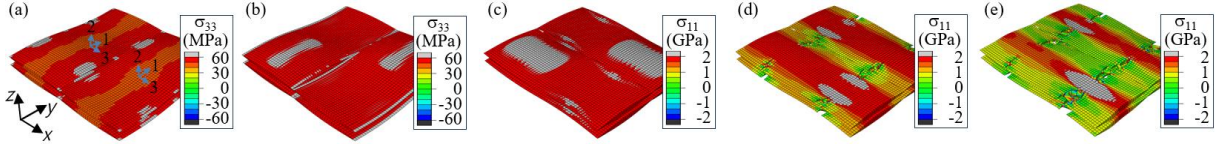
Figure 6. Failure propagation history in warp and fill tows: (a) $\bar{\varepsilon}_{xx} = 0.0046$, (b) $\bar{\varepsilon}_{xx} = 0.0066$, (c) $\bar{\varepsilon}_{xx} = 0.0136$, (d) $\bar{\varepsilon}_{xx} = 0.0148$, and (e) $\bar{\varepsilon}_{xx} = 0.0150$. (In a-b, only fill tows are shown, and in c-e only warp tows are shown.)
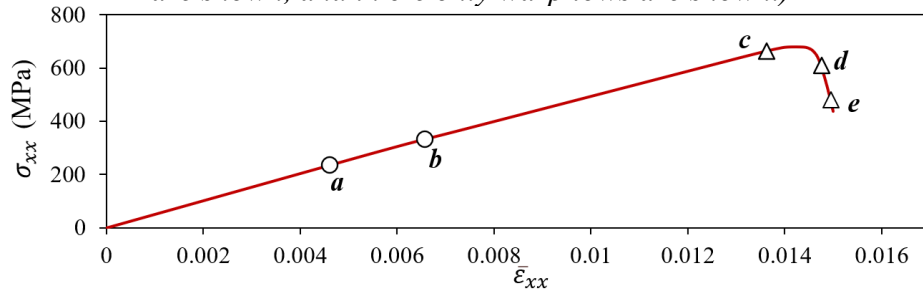
Figure 7. Nominal stress-strain curve under tension in the x-direction.

(3) Effective material property change. The internal structure of the plain weave unit cell changes during the failure propagation, resulting in changes the in-situ effective properties. The variations of effective tangential modulus and Poisson's ratio versus the applied tensile strain are shown in Figure 8. As discussed above, the tangential modulus shows the first decrease when fill tows fail between a and b in Figure 7. Then the tangential modulus decreases significantly as the warp tows fail which leads to the final failure between c and e. The effective Poisson's ratios also undergo similar variation, changing significantly first in strain range between a and b and then in strain range between c and e in Figure 7. In particular, during the final failure stage, the Poisson's ratios drop almost vertically because the nominal strain in the x-direction continuously increase, while those in the y- and z-direction remain almost unchanges.
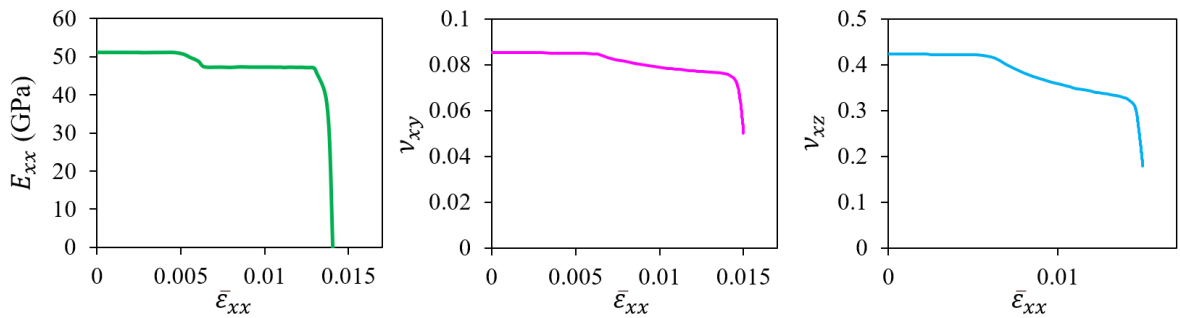
Figure 8. Variation of tangential modulus and Poisson's ratios.

CONCLUSION.

- An MPC-controlled selective activation of CZM was developed and applied to the progressive failure analysis of textile composite unit cell;
- MPC-controlled CZM method accurately predicted progressive failure results compared to experimental results and conventional CZM results;
- Under uni-axial tension load, the first failure occurred in fill tows in the matrix direction, but the final failure occurred in warp tows in the fiber direction;

- The tangential modulus and Poisson's ratios varied significantly depending on the failure progression of fill tows and warp tows.

REFERENCES:

1. A.C. Long, Design and manufacture of textile composites, Woodhead Publishing Limited, Cambridge, England, 2005.
2. A.P. Mouritz, M.K. Bannister, P.J. Falzon, K.H. Leong, Review of applications for advanced three-dimensional fiber textile composites, Composites Part A: Applied Science and Manufacturing, Vol. 30, Iss. 12, 1999, pp. 1445-1461.
3. P. Lozylo, Experimental-numerical study into the stability and failure of compressed thin-walled composite profiles using progressive failure analysis and cohesive zone model, Composite Structures, Vol. 257, 2021, 113303.
4. W. Zhang, Y. Huang, Three-dimensional numerical investigation of mixed-mode debonding of FRP-concrete interface using a cohesive zone model, Construction and Building Materials, Vol. 350, 2022, 128818.
5. N. Blal, L. Daridon, Y. Monerie, S. Pagano, Artificial compliance inherent to the intrinsic cohesive zone models: criteria and application to planar meshes, International Journal of Fracture, Vol. 178, 2012, pp. 71-83.
6. G.H. Paulino, W. Celes, R. Espinha, Z. Zhang, A general topology-based framework for adaptive insertion of cohesive elements in finite element meshes, Engineering with Computers, Vol. 24, 2008, pp. 59-78.
7. K. Woo, D.S. Cairns, Selective activation of intrinsic cohesive elements for fracture analysis of laminated composites, Composite Structures, Vol. 210, 2019, pp. 310-320.
8. S.C. Garcea, Y. Wang, P.J. Withers, X-ray computed tomography of polymer composites, Composite Science and Technology, Vol. 156, 2018, pp. 305-319.
9. M.L. Benzeggagh, M. Kenane, Measurement with mixed-mode delamination fracture toughness of unidirectional Glass/epoxy composites with mixed-mode bending apparatus, Composites Science and Technology, Vol. 56, No. 4, 1996, pp. 439-449.

ENHANCING ENERGY EFFICIENCY ENCLOSING STRUCTURES IN ADMINISTRATIVE BUILDINGS

RASHIDOV J (TUACE)

Abstract. *Nowadays administrative buildings being a significant part of the urban landscape, consume substantial amounts of energy for heating, cooling, and lighting. This research paper investigates methods to enhance the energy efficiency of administrative buildings, focusing on the critical role of the building's enclosing structures.*

Аннотация. *На сегодняшный день административные здания составляющие значительную часть городской экосистемы потребляют значительное количество энергии для отопления, охлаждения и освещения. В данной статье исследуются методы повышения энергоэффективности административных зданий, уделяя особое внимание важной роли ограждающих конструкций здания.*

Annotatsiya. *Bugungi kunda shahar ekotizimining muhim qismini tashkil etuvchi ma'muriy binolari isitish, sovutish va yoritish uchun katta miqdorda energiya manbalari sarflanadi. Ushbu maqolada ma'muriy binolarning energiya samaradorligini oshirish usullarini o'rganilib unda to'siq konstruksiyalarning muhimligiga e'tibor qaratiladi.*

Keywords: *Administrative buildings, climate zones, enclosing structures, energy efficiency, optimal design, thermal performance, sustainable construction.*

Ключевые слова: *Административные здания, климатические зоны, ограждающие конструкции, энергоэффективность, оптимальное проектирование, тепловые характеристики, экологичное строительство.*

Kalit so'zlar: *Ma'muriy binolar, iqlim zonalari, to'siq konstruksiyalar, energiya samaradorligi, optimal loyihalash, issiqlik ko'rsatkichlari, ekologik qurilish.*